



AIRNOISEUAM: An Urban Air Mobility Noise-Exposure Prediction Tool

Jinhua Li¹
University Space Research Association
Moffett Field, California, USA

Yun Zheng²
Crown Consulting Inc.
Moffett Field, California, USA

Menachem Rafaelof³
National Institute of Aerospace
Hampton, Virginia, USA

Hok Ng⁴
NASA Ames Research Center
Moffett Field, California, USA

Stephen A. Rizzi⁵
NASA Langley Research Center
Hampton, Virginia, USA

ABSTRACT

A new software tool called AIRNOISEUAM is introduced that models the noise exposure of Urban Air Mobility (UAM) operations. Given relevant UAM aircraft performance models, mission profiles, and Noise-Power-Distance data, AIRNOISEUAM predicts the noise exposure footprint for receptors on the ground. The performance of AIRNOISEUAM using a Robinson R66 helicopter model and a six-passenger quadrotor model, and a diverse set of scenarios from NASA’s UAM human-in-the-loop simulations is compared to that of the industry-standard tool with the same inputs. The predicted noise exposure results from both tools are found to be nearly identical. AIRNOISEUAM offers a fast-time, flexible interface and modular design to facilitate the dynamic requirements of the aviation research community.

1. INTRODUCTION

It is anticipated that Urban Air Mobility (UAM) will introduce a new class of electric Vertical Take-Off and Landing (eVTOL) vehicles such as “quadrotor” and “lift plus cruise” configurations operating in urban areas [1]. Effective mitigation of the noise generated by eVTOL operations will

¹ jinhua.li@nasa.com

² yun.zheng@nasa.com

³ menachem.rafaelof@nasa.gov

⁴ hokkwan.ng@nasa.gov

⁵ stephen.a.rizzi@nasa.gov

be critical to public acceptance of UAM operations. The industry-standard tool for modeling noise exposure near airports is the FAA’s Aviation Environmental Design Tool (AEDT) software [2]. The AEDT software cannot predict eVTOL noise exposure directly because it lacks both Noise-Power-Distance (NPD) data and performance models for eVTOL vehicles. A comprehensive survey of the current status and gaps for UAM noise prediction can be found in the past work [3].

The co-authors used NASA’s second-generation Aircraft Noise Prediction Program (ANOPP2) [4] software to estimate the NPD data of concept eVTOL vehicle models. Next, they used AEDT’s fixed-point profile method of fixed-wing aircraft to predict the eVTOL noise exposure [5].

This paper describes a new software tool called AIRNOISEUAM. AIRNOISEUAM was built on the previous software AIRNOISE [6][7] but developed to capture and account for the unique attributes of eVTOL operations in an urban environment. AIRNOISEUAM couples the same noise-exposure modeling method as AEDT. Different from AEDT developed for conventional aviation noise exposure assessment at the airport for the FAA’s noise compliance planning and regulations, AIRNOISEUAM is developed for the eVTOL noise research community with the following benefits:

1. Fidelity: The tool was based on the same noise-exposure modeling methods as the FAA’s benchmark aviation noise tool AEDT.
2. Efficiency: The core acoustic computation was written in high-level C language. Single noise event calculation can be performed in milliseconds.
3. Flexibility: All internal logic with parameters can be configured. Modular design allows easy integration with trajectory optimization software and UAM traffic management platforms.

The rest of the paper is organized as follows. Background on the state-of-the-art tools and methods is provided in Section 2. The software functions are presented in Section 3. A summary of the method and tools used to create the NPD data for passenger-carrying eVTOLs is presented in Section 4. The results for exposure-based metrics from AIRNOISEUAM are presented in Section 5 and compared against those obtained from AEDT. Concluding remarks and future work are presented in Section 6.

2. BACKGROUND

The Aviation Environmental Design Tool (AEDT) software is the FAA-mandated tool for National Environmental Policy Act (NEPA) studies if federal actions are involved. The AEDT mainly uses the empirical methods recommended by the SAE International to calculate noise exposure resulting from both fixed-wing aircraft and helicopter operations. As defined in SAE-AIR-1845 [8], the method calculates noise exposure by interpolating Noise-Power-Distance (NPD) data with engine power and distance to the receptor. The NPD data is derived from aircraft certification sound exposure data at a standard atmospheric condition. The noise exposure at the receptor then accounts for atmospheric propagation and includes adjustments for vehicle speed, lateral attenuation, and noise fraction to account for finite-segment representation of flight profiles at other atmospheric conditions.

The SAE-AIR-1845 document describes procedures for calculating Sound Exposure Level (SEL) at a receptor, resulting from a departure or an arrival aircraft operation. More precisely, the SEL resulting from a flight segment is calculated by adding together a base noise value with several adjustment terms [2][8], as follows:

$$L_{ae} = L_{ae}(P, d) + ADJ_{NF} + ADJ_{DUR} - ADJ_{LA} \quad (3-1)$$

Here, $L_{ae}(P, d)$ represents A-weighted SEL from NPD data. For fixed-wing aircraft, P represents engine power. For helicopter and eVTOL, P represents the vehicle operating state.

The NPD data values are measured under the conditions of a straight overhead flight and adjusted for a constant speed of 160 knots at standard atmospheric conditions. The rest of the terms in Equation 3-1 account for adjustments. Specifically, noise fraction ADJ_{NF} adjusts for the finite-length flight path segment; noise duration ADJ_{DUR} represents the adjustment due to aircraft speed; and noise lateral attenuation ADJ_{LA} adjusts for the receptor’s lateral deviation from the flight path. Other nonlinear adjustments such as surface elevation are not listed in (3-1), but they are incorporated in AIRNOISEUAM. Adjustments for the vehicle’s ground operations are not considered in this work.

The SEL value for a single flight segment is calculated using Equation 3-1, while the SEL value for multiple segments is then calculated using:

$$L_{ae,flt} = 10 \log_{10} \left(\sum_{i=1}^{N_{seg}} 10^{\frac{L_{ae,i}}{10}} \right) \quad (3-2)$$

where $L_{ae,i}$ is the SEL of the i^{th} segment obtained using Equation 3-1; and N_{seg} is the total number of segments.

Lastly, Day-and-Night Average Sound Level (DNL) is the most important FAA compliance planning regulation metric at the airport. It is calculated as follows:

$$L_{dn} = \sum_{flt \in day} 10^{\frac{L_{ae,flt}}{10}} + \sum_{flt \in night} 10^{\frac{L_{ae,flt}+10}{10}} - 49.4 \quad (3-3)$$

where nighttime is defined from 10p.m. to 7a.m. local time. DNL considers the time of day of an aircraft operation and applies a 10dB penalty on aircraft that arrive or depart at night.

3. SOFTWARE MODELING FUNCTIONAL OVERVIEW

Figure 1 depicts the notional system architecture of the AIRNOISEUAM tool. The main modules shown in the system architecture and their primary functions are as follows:

- airnoiseUAM:** This module computes sound exposure using the SAE-AIR-1845 method, given the flight profile data as input. The flight profile data must include vehicle type, flight profile (latitude, longitude, altitude, and speed), and operating states. This module also includes a library of Python scripts for validation and plotting.
- Gen-1.2 NPD data:** The NPD data contain eVTOL aircraft sound exposure levels and the maximum A-weighted sound pressure levels simulated using ANOPP2 for a set of vehicle operating states and distances to the receptor at standard atmospheric conditions.
- airnoiseProfile:** This module converts flight plan and flight trajectory data from outside into the fixed-point flight profile input data required by airnoiseUAM.
- airnoiseMap:** This module contains routines used to interactively visualize vertiports, airspace infrastructure, and local noise-sensitive land uses, overlaid with noise exposure contours predicted using airnoiseUAM.
- airnoiseAnalytics:** This module applies machine learning algorithms to analyze and predict the noise compliance and impact on local communities.

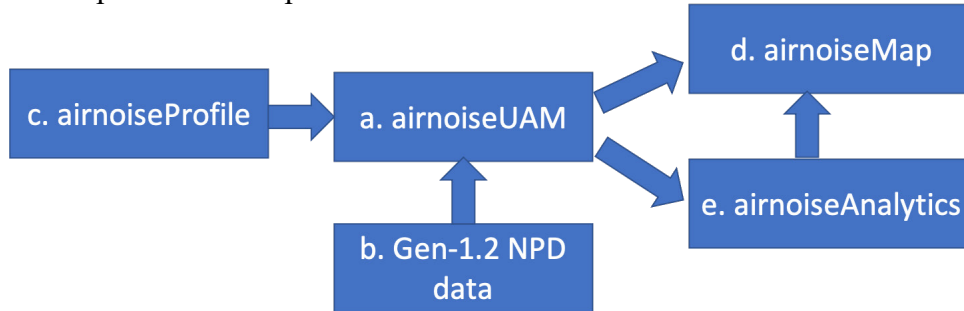


Figure 1: Notional system block diagram of AIRNOISEUAM

The focus of this paper is mainly on the airnoiseUAM module and, to a lesser extent, the generation and use of Gen-1.2 NPD data in Figure 1. Please refer to [9] for the work on developing airnoiseMap and companion paper [5] on developing Gen-1.2 NPD data and using AEDT's fixed-point profile method of fixed-wing aircraft to predict noise exposure of UAM vehicles.

4. GEN-1.2 NOISE-POWER-DISTANCE DATA

Simulation data from sixteen routes around the Dallas-Fort Worth area were provided by NASA's human-in-the-loop UAM engineering simulation group [10]. Because the NPD data were numerically estimated using ANOPP2 (versus the customary practice of deriving NPD data from measurements), and that process is computationally intensive, the number of operating conditions evaluated were necessarily fewer than higher sampling rate (1-Hz) 4D data utilized in the route simulation. The route simulation data were examined from the most prevalent operating conditions, specified as a combination of airspeed and climb angle. A unique numerical identifier, e.g., 101, 102, etc., was used to identify the particular operating condition or state, and the particular condition used was prescribed on a segment-wise basis using the fixed-point flight profile mode within AEDT [2].

The same approach was adopted for AIRNOISEUAM. In this respect, the performance model within AEDT was bypassed and the “P” (power) in NPD was used to designate the operating condition. Using this process, NPD data were generated for a total of 42 unique operating conditions for the NASA Revolutionary Vertical Lift Technology (RVLT) project quadrotor reference concept vehicle [1].

The overall process is depicted in Figure 2. Given the vehicle configuration and prescribed condition (again, the “P” identifier in NPD), the vehicle is “trimmed” in an iterative fashion using a comprehensive analysis code. In the trimmed condition, the control surface configuration of the vehicle corresponds to the desired flight condition. For this work, the Comprehensive Analytical Model of Rotorcraft Aerodynamics and Dynamics (CAMRAD II) [11-13] was used to trim the vehicle. The resulting blade loadings and motion serve as input to the system noise prediction software. In this work, the system noise prediction was computed using ANOPP2’s AeroAcoustic Rotor Noise (AARON) tool. The acoustics solver uses Farassat’s Formulation F1A [14] to compute the periodic loading and thickness noise components only under a quasi-static operating condition. These two components constitute the so-called first generation (Gen-1.2) database. Subsequent generations will include additional noise components. The resulting source noise definition is subsequently “flowed” at the 160-knot AEDT reference speed at different distances (the “D” in NPD) above an observer under the flight path, and the requisite noise metrics (the “N” in NPD) are calculated using ANOPP2’s Acoustic Analysis Utility. Additional details on the NPD generation process can be found in the companion paper [5].

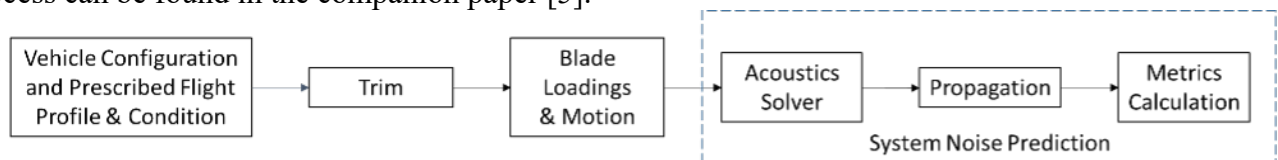


Figure 2. The general process for predicting the periodic loading and thickness noise components in the Gen-1.2 NPD database.

5. VALIDATION WITH AEDT

In this section, the predicted noise exposure resulting from individual flight segments and integrated scenarios are compared against those obtained from AEDT. The companion paper [5] presents a method to use the fixed-point profile method of fixed-wing aircraft to predict noise exposure of UAM vehicles in AEDT. Sections 5.1 and 5.2 use a Robinson R66 helicopter model. Section 5.1 compares noise exposure predictions resulting from a single flight segment, while Section 5.2 compares noise exposure predictions resulting from multiple flight segments. Section 5.3 and Section 5.4 use a more complicated six-passenger quadrotor model developed by Silva and Johnson [1]. Section 5.3 compares exposure predictions resulting from a full flight route, while Section 5.4 computes the DNL predictions resulting from 16 flight routes obtained from NASA’s UAM human-in-the-loop simulation.

5.1 COMPARISON FOR A SINGLE SEGMENT WITH R66 HELICOPTER MODEL

The first test case models a six-passenger Robinson R66 helicopter flying the flight profile shown in Figure 3. The flight profile, derived from a sizing mission profile [1], was further divided into short segments for comparison. The R66 NPD data used in this comparison was calculated according to the method described in Section 4. Within AEDT, the fixed-point flight profile method described in [2][5] - instead of the AEDT helicopter mode - was used. The main test conditions are listed below:

- Two receptor grid arrays were defined. A coarse grid set was used for comparisons in the climb, cruise, and descent segments. The size of each coarse grid was 800 ft by 800 ft. A fine grid set was used for comparisons in vertical hover, horizontal hover, vertical ascent, and vertical descent segments. The size of each fine grid was 40 ft by 40 ft.
- Atmospheric absorption adjustment was not applied.
- Overall, lateral attenuation was disabled; that is, ground effects, refraction scattering effects, and engine installation effects were not modeled.

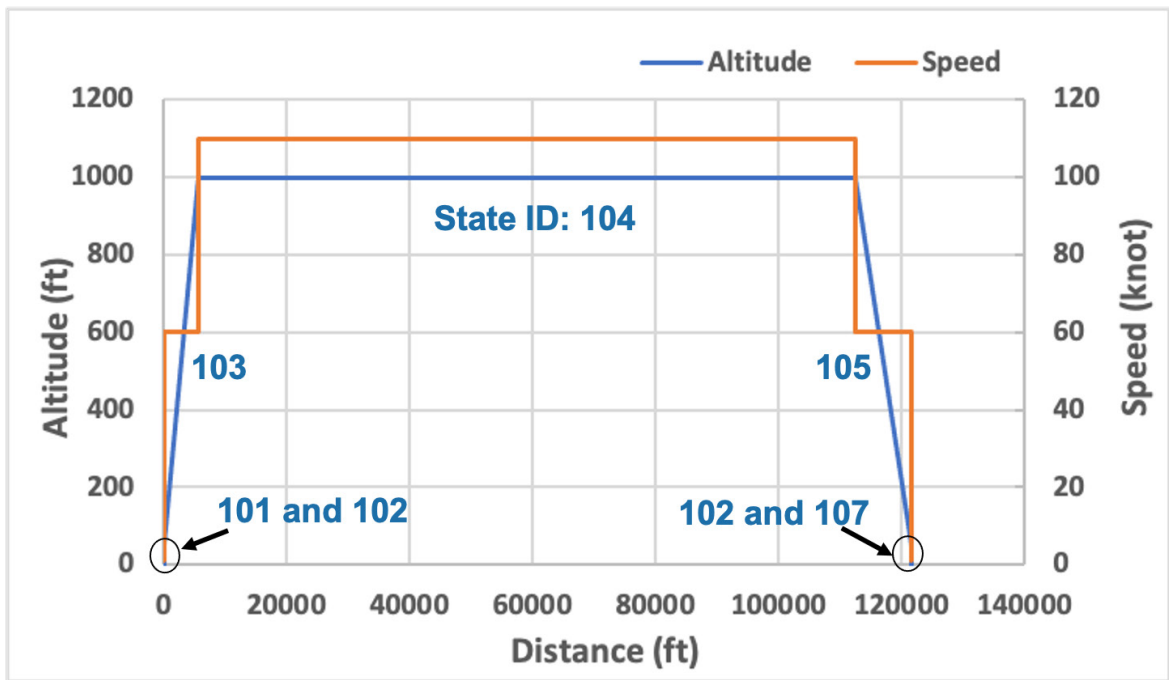


Figure 3. Flight profile of a six-passenger R66 helicopter with 7 operating states (State ID 101: vertical ascent, 102: horizontal hover and vertical hover, 103: climb, 104: cruise, 105: descent, and 107: vertical descent)

First, performance was compared along seven individual segments. Each segment represented a unique flight operating state: horizontal hover, vertical hover, vertical ascent, vertical descent, cruise, climb, or descent. The horizontal and vertical hover states were two means of representing hover and include a small amount (typically about 1 ft./sec.) of horizontal and vertical motion, respectively. The results are shown in Figure 4.

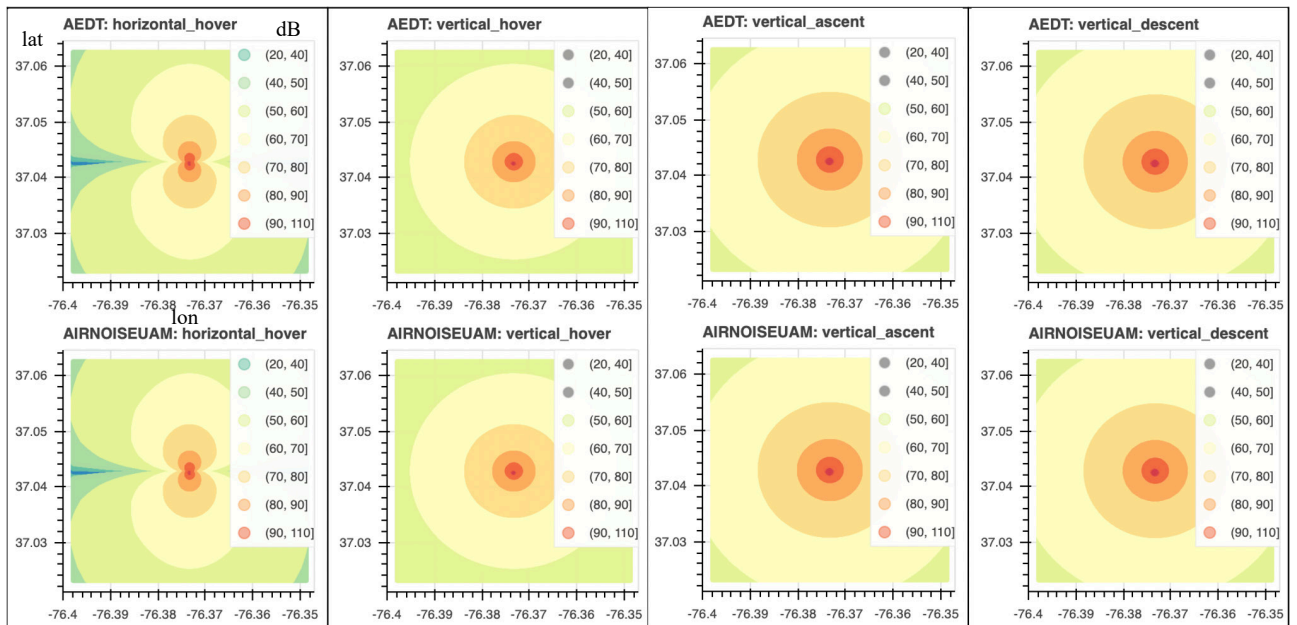


Figure 4-1. Single flight segment sound exposure level values (dB) for different flight operating states (from left to right: horizontal hover, vertical hover, vertical ascent and vertical descent) predicted using AEDT (top row) and AIRNOISEUAM (bottom row)

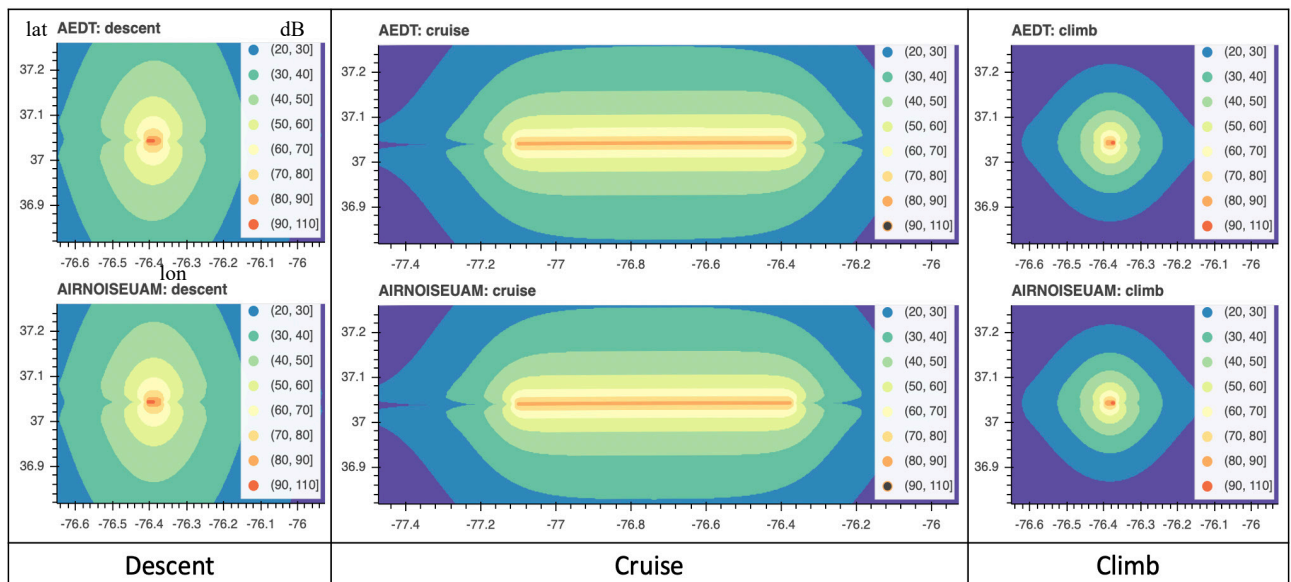


Figure 4-2. Single flight segment sound exposure level values at different flight operating states (from left to right: descent, cruise, and climb) predicted using (top row) AEDT and (bottom row) AIRNOISEUAM

Figure 4 and Table 1 illustrate how well the implementation in AIRNOISEUAM compared with the fixed-point flight profile method for fixed-wing aircraft within AEDT. Figure 4 shows that the predicted noise contour from AIRNOISEUAM accurately captures the predicted noise contour characteristics from AEDT. Table 1 further compared the sound exposure predictions at the receptors. The maximum difference at all receptors is less than 2dB, while it is commonly accepted that a 3dB sound exposure level difference is barely perceivable to most human ears. It shows that the results are practically the same on all seven flight segments.

Table 1: Difference between the AIRNOISEUAM and AEDT results at receptors

Segment	State ID	Average receptor SEL differences	Min SEL differences	Max SEL differences
Vertical Ascent	101	0.07 dB	0.07 dB	0.08 dB
Horizontal Hover	102	0.08 dB	0.07 dB	1.82 dB
Vertical Hover	102	0.07 dB	0.07 dB	0.08 dB
Climb	103	0.07 dB	0.03 dB	0.12 dB
Cruise	104	0.09 dB	0.0 dB	1.49 dB
Descent	105	0.12 dB	0.00 dB	1.97 dB
Vertical Descent	107	0.07 dB	0.07 dB	0.08 dB

5.2 COMPARISON FOR A BASELINE STUDY WITH R66 HELICOPTER MODEL

The second test case used a full flight profile of the R66 helicopter model. The main test conditions are listed below:

- The size of the receptor grid set was 0.05 mile by 0.05 mile.
- Horizontal and vertical hover states were not included.
- Vehicle ground operations were not considered.
- Bank angle was set to zero.
- Noise lateral attenuation adjustment and duration attenuation adjustment were applied.
- Each flight segment was associated with an operating state. The operating state was defined by a combination of airspeed and climb angle.

There were five flight segments in this test case:

- *SegA*: vertical ascent, state ID = 101

- *SegB*: climb, state ID = 103
- *SegC*: cruise, state ID = 104
- *SegD*: descent, state ID = 105
- *SegE*: vertical descent, state ID = 107

Three tests were conducted, as follows:

- Climb test: *SegB*
- Vertical ascent test: *SegA_NearVert-B*
- Full route test: *SegA-E_v0*

There is a key implementation difference between AIRNOISEUAM and AEDT, in the case where the operating states are different between the starting point and the ending point of a flight segment. AIRNOISEUAM uses the operating state at the starting point as the segment operating state. Because the test uses a fixed-point profile method of fixed-wing aircraft in the AEDT, a “guard” point is added just prior (typically 12 ft) to the beginning of the next segment to avoid NPD data interpolation between two different operating states over most of the segment length. Interpolation is still performed within AEDT over the 12-ft transition segment. Additional detail may be found in the companion paper [5].

Table 2 summarizes the results. The average difference is close to zero decibels on all three tests. The maximum difference is 1.3 decibels over all receptors. Also, the average SEL difference for single segment was lower as compared to the results in Table 1 as a result of incorporating acoustic impedance adjustment.

Table 2. Difference between the AIRNOISEUAM and AEDT results at receptors

Segment	States	Average SEL differences per receptor	Min SEL differences	Max SEL differences
<i>SegB</i>	103	0.014 dB	0.008 dB	0.025 dB
<i>SegA_NearVert-B</i>	101, 103	0.006 dB	0.0 dB	0.031 dB
<i>SegA-E_v0</i>	101, 103, 104, 105, 107	0.04 dB	0.0 dB	1.29 dB

Figure 5 shows the noise contours of climb segment *SegB* for AEDT (left) and AIRNOISEUAM (right). The results are visually indistinguishable, as shown in Table 2.

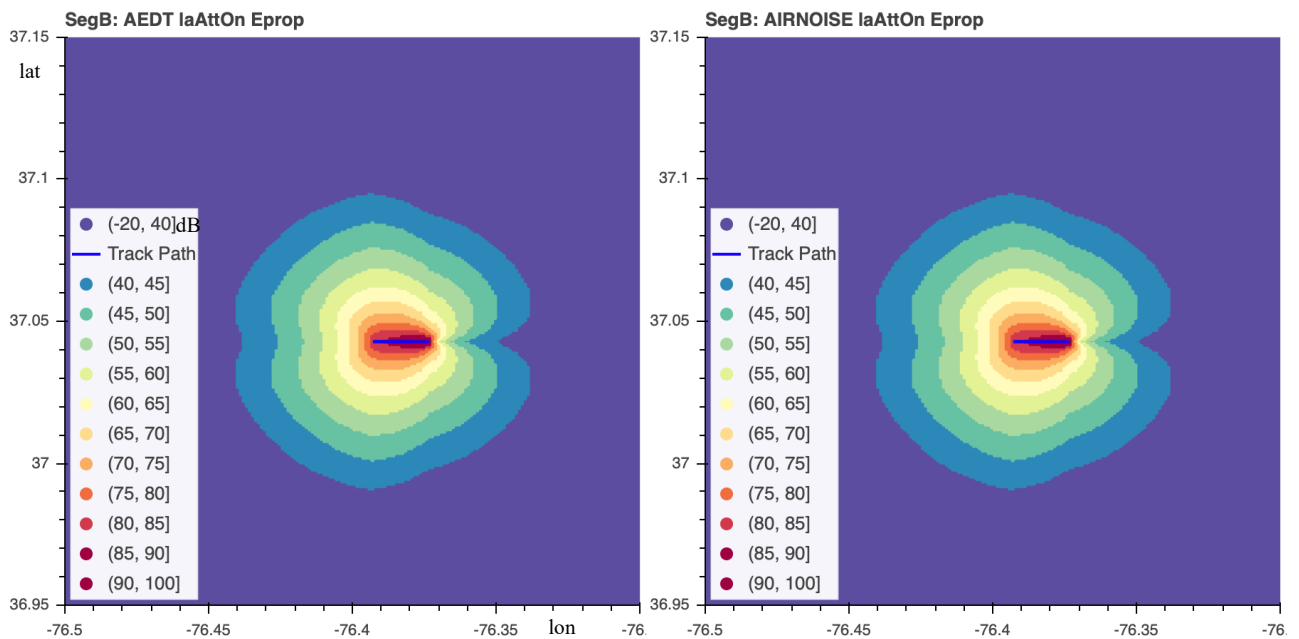


Figure 5. Single climb segment *SegB* test results predicted using AEDT (left) and AIRNOISEUAM (right)

Lastly, Figure 6 shows noise exposure results from a full flight profile: SegA-E_v0. Note that the landing area on the left side of the figure has elevated noise-exposure levels relative to the cruise and takeoff segments to the right (i.e., east) of the landing area. This is due to higher noise levels associated with descent.

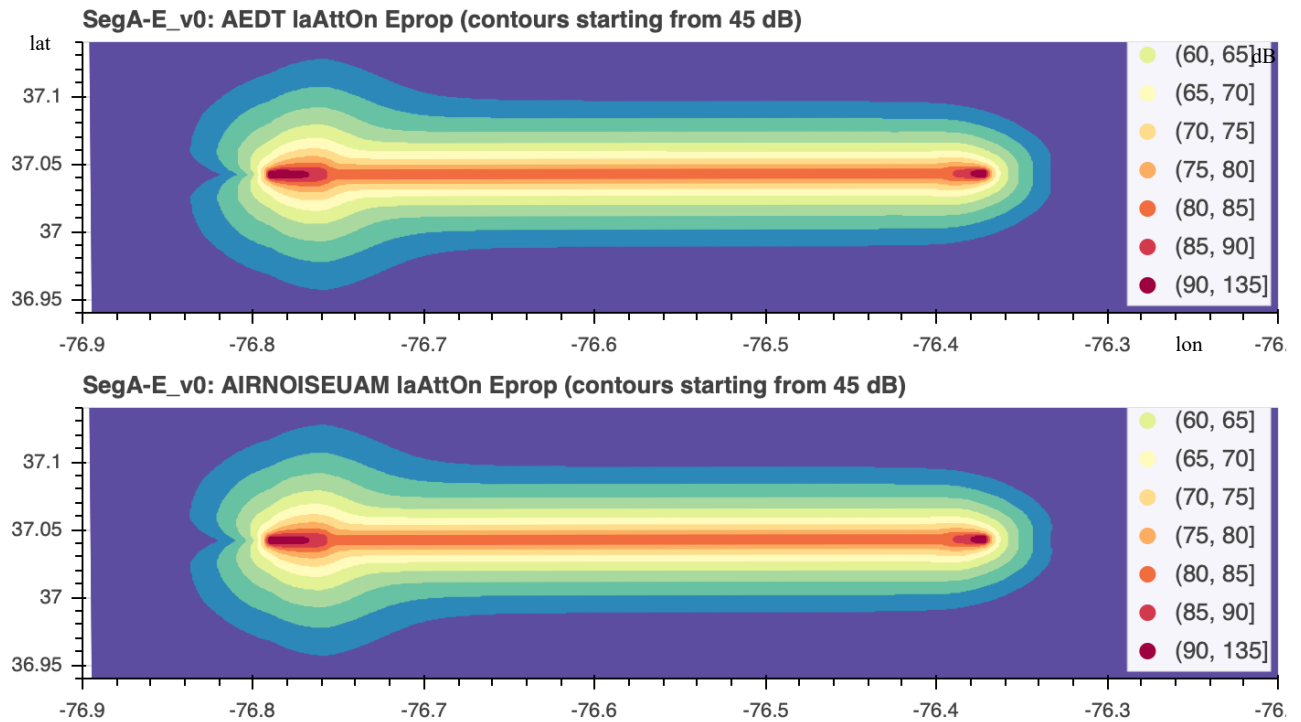


Figure 6. Test results of a full flight profile from AEDT (top) and AIRNOISEUAM (bottom). Direction of flight is from right (east) to left (west).

5.3 COMPARISON FOR A PROPOSED UAM ROUTE WITH QUADROTOR MODEL

In this test case, a prototype six-passenger electric quadrotor is used based on the concept model developed in [1]. A rendered vehicle is shown in Figure 7. The flight route was modeled based on subject-matter expert elicitation [10]. The vertical profile for the route is shown in Figure 8. The flight profiles for this test case are significantly more complicated than the simplified case undertaken in Section 5.2. In particular, as detailed in Section 4, 42 distinct operating states and NPD tables were generated and used for quadrotor for quadrotor versus 7 distinct operating states for R66. Please refer to companion paper [5] for detail regarding the construction of the quadrotor flight profile.



Figure 7. A rendered image of a 6-passenger quadrotor

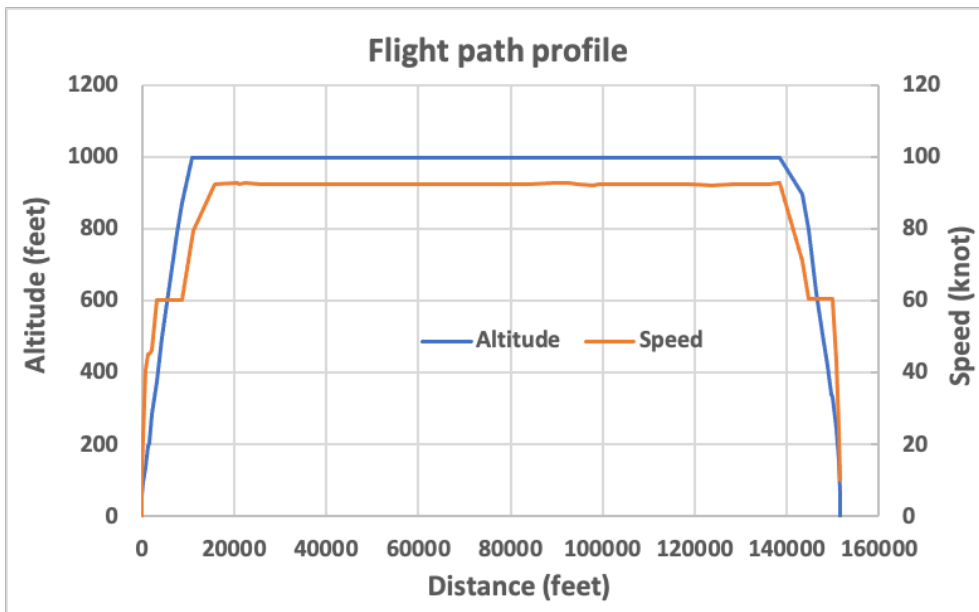


Figure 8. Vertical flight profile modeled for the six-passenger electric quadrotor. Twenty-nine of the quadrotor’s 42 unique operating states were used for this route.

Figure 9 presents the results from one of the sixteen modeled routes. The average difference in noise exposure was 0.14 decibels, while the maximum difference at any receptor was less than 1.4 decibels. More specifically, 99.88 percent of receptors reported a noise difference of less than 0.5 decibels, and 99.99% of receptors reported a noise difference of less than 1 decibel.

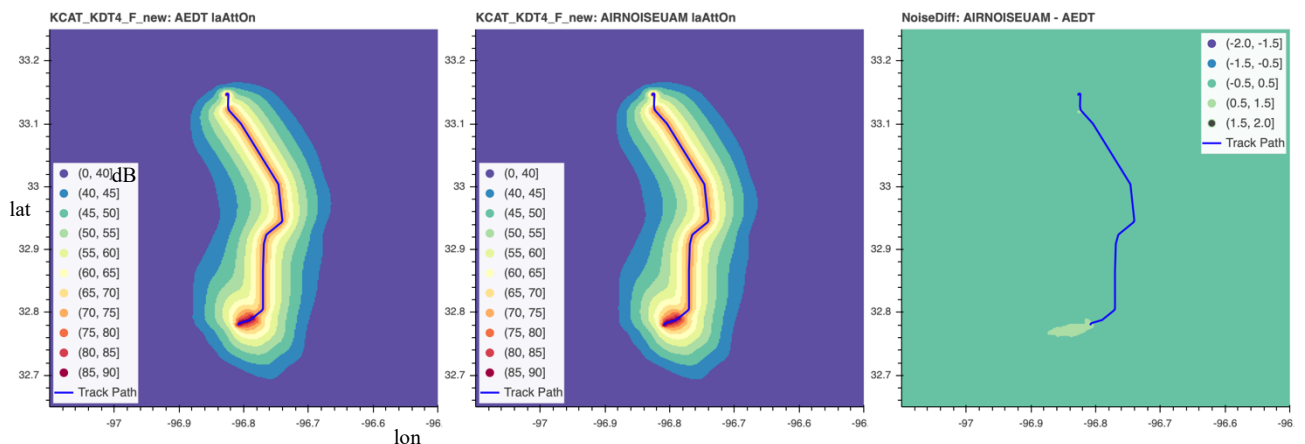


Figure 9. Sound exposure level values for a full flight profile of an electric six-passenger quadrotor flying along a proposed UAM route modeled with AEDT (left) and AIRNOISEUAM (middle). At right are depicted their resulting differences at the receptors.

5.4 COMPARISON FOR SIXTEEN PROPOSED UAM ROUTES WITH QUADROTOR MODEL

Figure 10 shows all sixteen routes for initial UAM operations in the Dallas-Fort Worth region. In this test case, both AIRNOISEUAM and AEDT were used to predict noise contours for all sixteen routes with a quadrotor model.

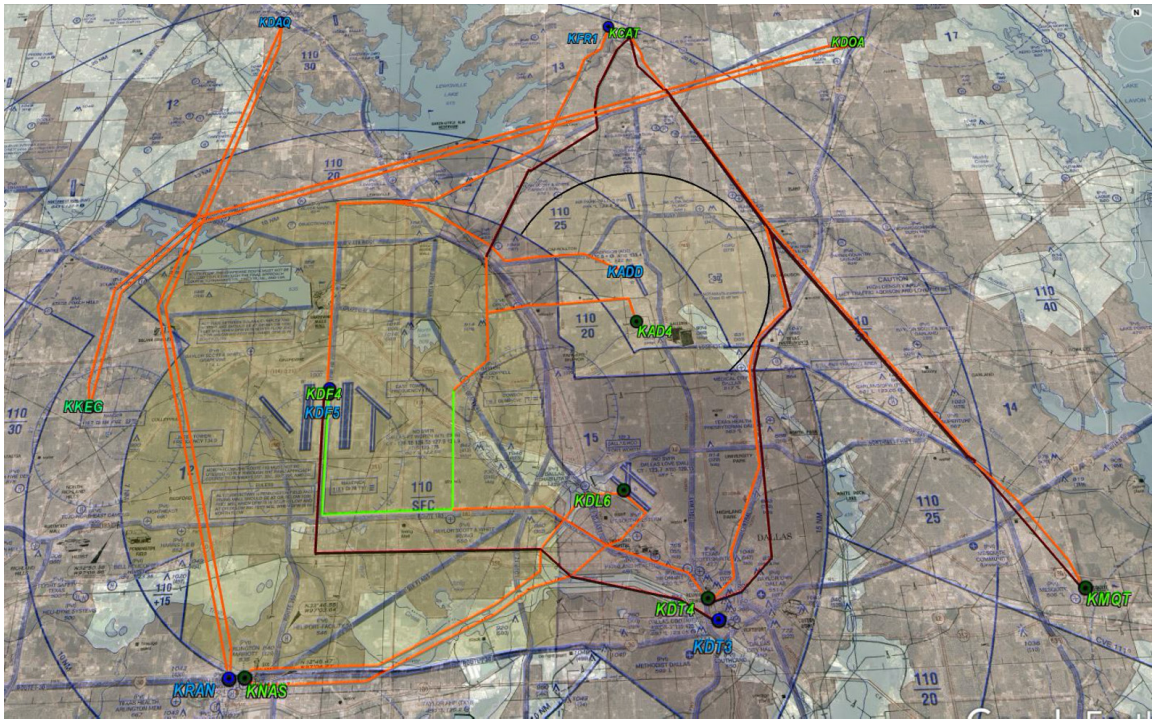


Figure 10. Sixteen routes proposed for initial UAM operations in the Dallas Fort-Worth region

Figure 11 shows the DNL contour results for all sixteen routes assuming 600 daytime operations per route. AIRNOISEUAM and AEDT produce nearly the same DNL contours with small differences near the vertiports, as shown in Fig. 12. Based on discussions with the AEDT development team at Volpe Research Center, we believe such differences are not due to modeling error but due to implementation differences between the two software tools for operations modeled near the surface.

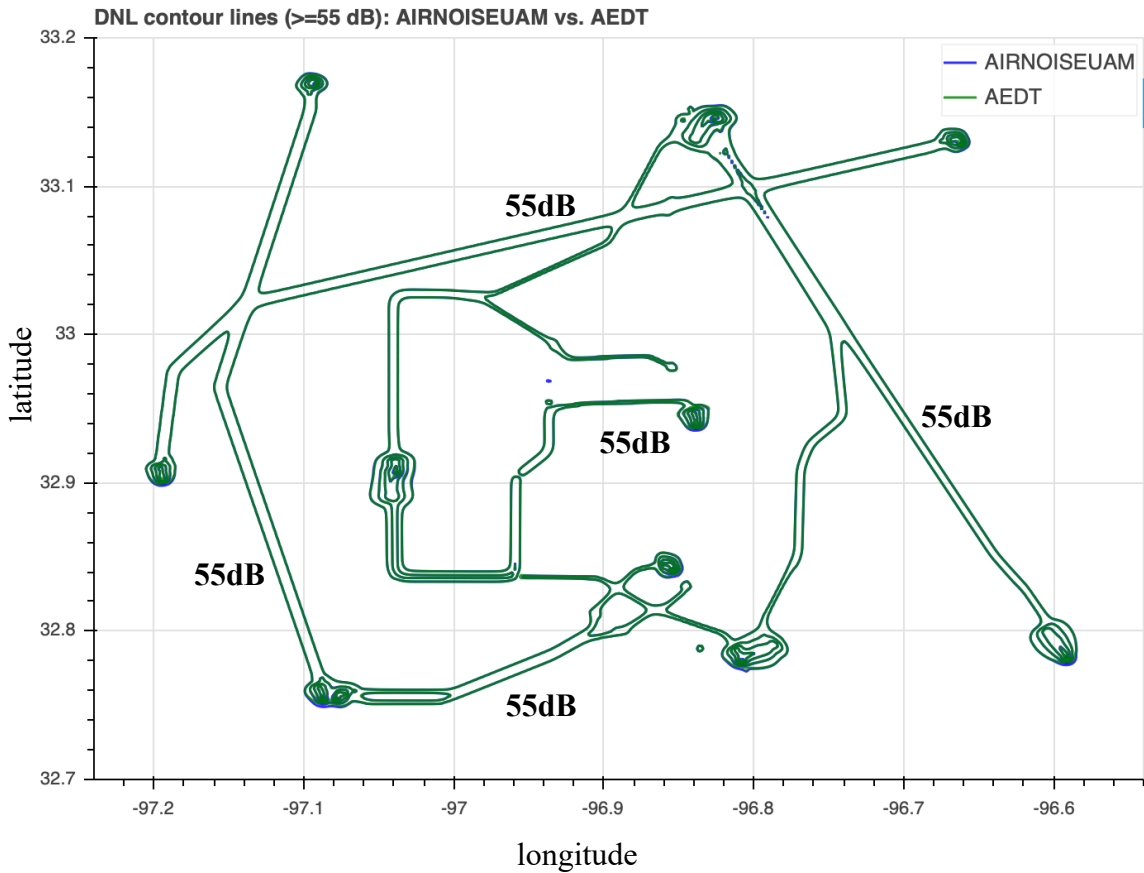


Figure 11. DNL contours (starting at 55 decibels with contour lines at 5-decibel increments) for sixteen proposed UAM routes in the Dallas-Fort Worth area, predicted using AIRNOISEUAM and AEDT

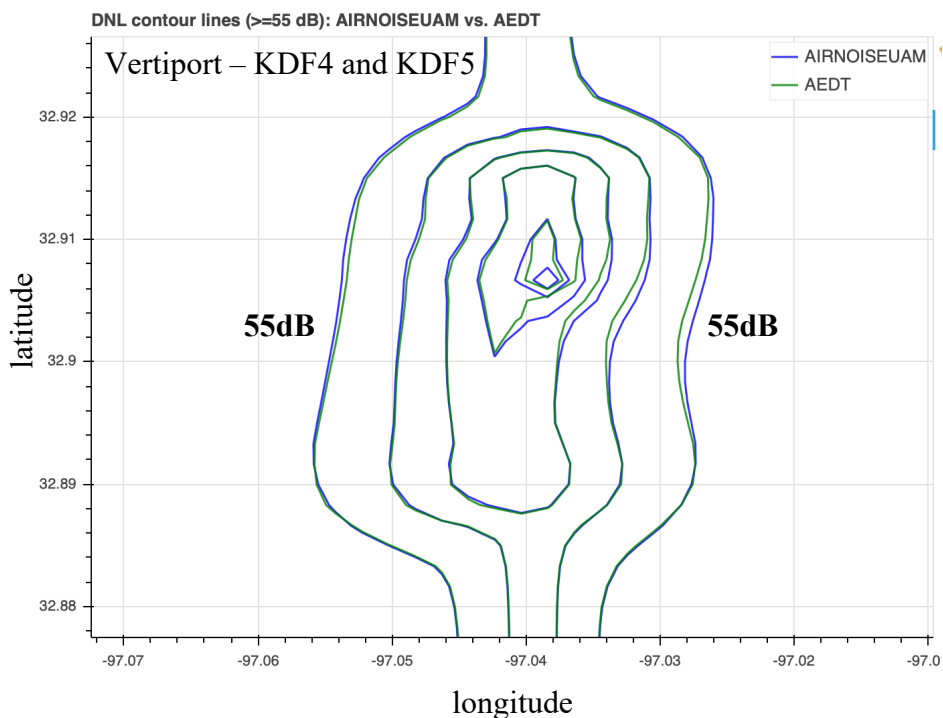
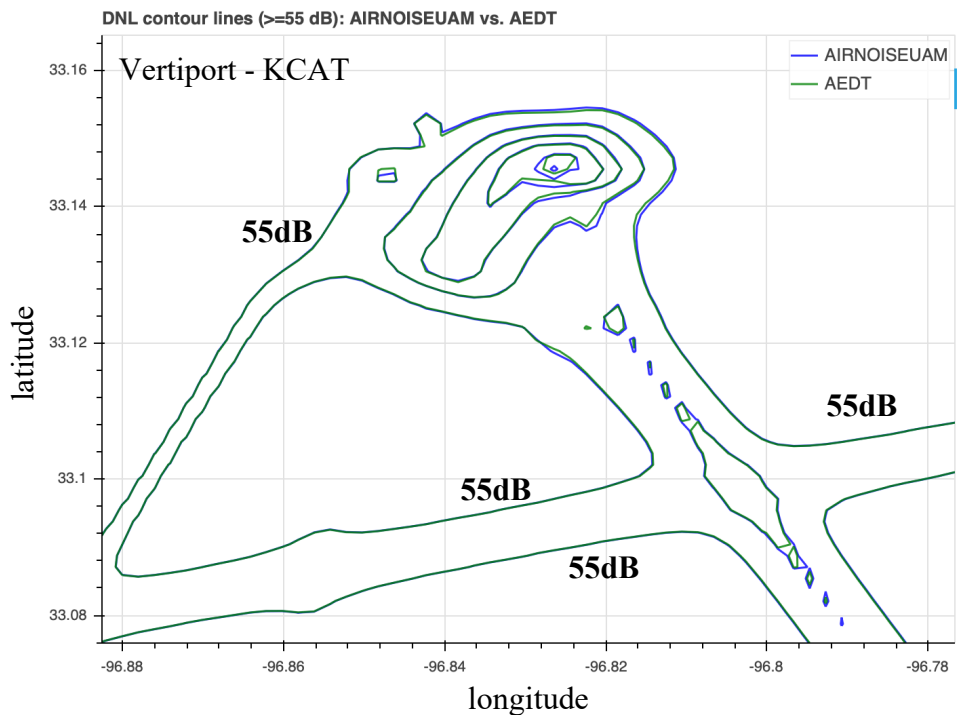


Figure 12. DNL contours (starting at 55 decibels with contour lines at 5-decibel increments) near two selected vertiports

In summary, such close results in all test cases validate that AIRNOISEUAM implemented the SAE-AIR-1845 procedures as closely as AEDT.

6. CONCLUSIONS AND FUTURE WORK

In this paper, a new tool, “AIRNOISEUAM,” was introduced for noise exposure prediction of Urban Air Mobility (UAM) vehicle operations. The AIRNOISEUAM implemented the method described in the SAE-AIR-1845 and AEDT documents for computing sound exposure of concept UAM vehicles with the Gen-1.2 NPD. The results for exposure-based metrics show very close agreement between predictions by the two software tools.

In future work, the airnoiseAnalytics module will be developed to apply the machine learning algorithms to analyze and predict the noise compliance and impact on local communities. The upcoming Gen-2 NPD data that improve noise prediction accuracy by incorporating broadband self-noise will be integrated into AIRNOISEUAM. The “AIRNOISEUAM” is designed to suit UAM noise research applications such as noise-mitigation route planning. The AIRNOISEUAM tool is currently being applied to large-scale UAM operation noise assessment using data from NASA’s ongoing slate of UAM human-the-loop simulations.

7. REFERENCES

1. Silva, C., Johnson, W., Antcliff, K.R. & Patterson, M.A., VTOL Urban Air Mobility Concept Vehicles for Technology Development, *2018 Aviation Technology, Integration, and Operations Conference*, AIAA-2018-3847 (2018).
2. Aviation Environmental Design Tool (AEDT), Version 3c, Technical Manual, Federal Aviation Administration, *DOT-VNTSC-FAA-20-05* (2020).
3. Rizzi, S.A., et. al, Urban Air Mobility Noise: Current Practice, Gaps, and Recommendations, *NASA Technical Publication 2020-5007433* (2020).
4. Lopes, L.V. and Burley, C.L., ANOPP2 User's Manual: Version 1.2, NASA TM-2016-219342 (2016).
5. Rizzi, S.A. & Rafaelof, M., Community noise assessment of urban air mobility vehicle operations using the FAA Aviation Environmental Design Tool, *InterNoise 2021*, Virtual Meeting (2021).
6. Li, J., Chen, N., Ng, H. & Sridhar, B., Simple tool for aircraft noise-reduction route design, *15th AIAA Aviation Technology, Integration, and Operation Conference* (2015).
7. Li, J., Sridhar, B., Xue, M. & Ng, H., AIRNOISE: a tool for preliminary noise-abatement terminal approach route design, *16th AIAA Aviation Technology, Integration, and Operation Conference* (2016).
8. The SAE International, Procedure for the calculation of airplane noise in the vicinity of airports, *SAE-AIR1845A* (2012).
9. Li, J., Ng, H., Zheng, Y. & Gutierrez, S., Noise exposure map of urban air mobility, *AIAA Aviation Forum and Exposition*, June (2021).
10. Verma, S. A., et. al, Lessons Learned: Using UTM Paradigm for Urban Air Mobility Operations, *AIAA/IEEE 39th Digital Avionics System Conference*, San Antonio, TX, October (2020)
11. Johnson, W., Technology Drivers in the Development of CAMRAD II, *American Helicopter Society Aeromechanics Specialist Meeting*, San Francisco, California, January (1994).
12. Johnson, W., Rotorcraft Aeromechanics Applications of a Comprehensive Analysis, *HeliJapan 1998: AHS International Meeting on Rotorcraft Technology and Disaster Relief*, Gifu, Japan, April (1998).
13. Johnson, W., Rotorcraft Aerodynamic Models for a Comprehensive Analysis, *American Helicopter Society 54th Annual Forum*, Washington, D.C., May (1998).
14. Farassat, F. & Succi, G. The Prediction of Helicopter Rotor Discrete Frequency Noise, *Vertica*, vol. 7, pp. 309-320 (1983).